RESEARCH ON LAMINAR SEPARATION BUBBLES AT DELFT UNIVERSITY OF TECHNOLOGY

by

J.L. van Ingen

In: "Separated Flows and Jets" IUTAM Symposium

Novosibirsk, USSR
1990
Eds: V.V. Kozlov, A.D. Dovgal

Note: This paper gives a review of research at Delft University of Technology on laminar separation bubbles. Results of flow visualisation studies are used to define an empirical relation for the angle at which the separation streamline leaves the wall. The e^N transition prediction method is extended to separated flows. A universal description of the laminar part of the bubble is proposed, resulting in a simple bubble prediction method.

Research on Laminar Separation Bubbles at Delft University of Technology

J.L. VAN INGEN

Department of Aerospace Engineering
Delft University of Technology
Kluyverweg 1, 2629 HS Delft, The Netherlands

Summary
This paper gives a review of research at Delft University of Technology on laminar separation bubbles. Results of flow visualisation studies are used to define an empirical relation for the angle γ at which the separation streamline leaves the wall. The "e-to-the-n" transition prediction method is extended to separated flows. A universal description of the laminar part of the bubble is proposed, resulting in a simple bubble prediction method.

1. Introduction

At the Low Speed Laboratory (LSL) of the Department of Aerospace Engineering of the Delft University of Technology a long term research program has been going on concerning the analysis and design of airfoil sections for low speed flow. For these flows the possible occurrence of laminar separation bubbles has a marked influence on the pressure distribution and on the development of the boundary layer downstream of the bubble. As an example Fig. 1 gives some results of pressure distribution measurements obtained at LSL for a Wortmann airfoil. Within the bubble a characteristic flattening of the pressure distribution can be noticed. At low Reynoldsnumbers (<.1 * 10^6 in Fig. 1) the turbulent flow may fail to reattach and "bursting" of the bubble is said to have occurred. It will be clear that any computer code, aimed at predicting the characteristics of airfoils at relatively low Reynoldsnumbers should be able to treat these separation bubbles. In a number of papers [1-5] the author and his colleagues have reported on studies at LSL regarding separation, transition and reattachment and also on the design of low Reynolds number airfoils.
A schematic description of the flowfield and the pressure distribution in the bubble region is given in Fig. 2.
Due to lack of space the present paper will only discuss the laminar part of the bubble (S-T) and transition (T). For discussions on reattachment the reader is referred to [1-5]. In most engineering calculation methods the

V.V. Kozlov, A.V. Dovgal (Eds.)
Separated Flows and Jets
IUTAM Symposium Novosibirsk/USSR 1990

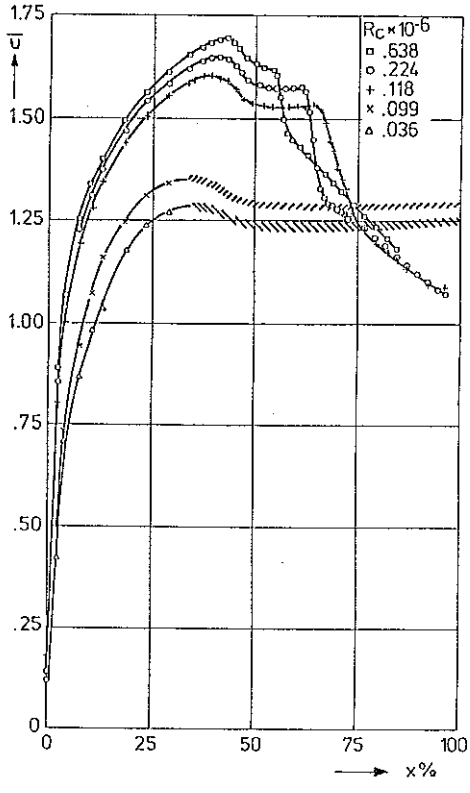

Fig. 1. Measured pressure distributions for the Wortmann FX66-S-196VI airfoil, $\alpha = 1^0$.

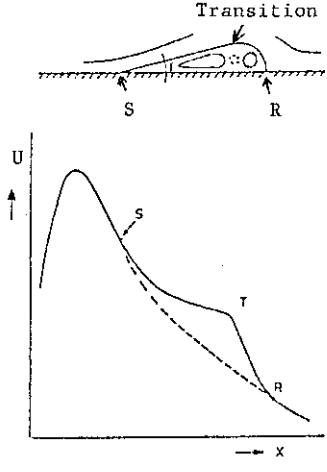

Fig. 2. Schematic diagram of flow field and pressure distribution in a laminar separation bubble.

pressure distribution in the bubble is treated as a local perturbation only of the pressure distribution curve SR which whould occur for a turbulent boundary layer. Hence the laminar separation point S and the reattachment point R are thought to be on the turbulent curve. In reality a slight undershoot is often noticed around S and R.

2. Some useful relations for separating laminar flow

In a small neighbourhood of the separation point, where the inertial forces may be neglected, the Navier-Stokes equations admit a simple analytical solution [6-8]. Important results are: The separation streamline leaves the wall at an angle γ (Fig. 2) which is determined by:

$$\tan(\gamma) = -3 \frac{dr_o}{dx} \Big/ \frac{\partial p}{\partial x} \qquad (1)$$

where all quantities in (1) are evaluated at the separation point (for nomenclature see section 8).
The equation for the streamlines reads:

$$y^2(x \tan \gamma - y) = \text{constant} \qquad (2)$$

where x is the distance downstream of separation.
The shear stress is zero at $y = y_1$ for which:

$$y_1 = \tfrac{1}{3} x \tan \gamma \qquad (3)$$

The velocity component u equals zero at y_2 for which:

$$y_2 = \tfrac{2}{3} x \tan \gamma \qquad (4)$$

Hence (when y_3 denotes the distance to the wall of the separation streamline):

$$y_1 : y_2 : y_3 = 1 : 2 : 3 \qquad (5)$$

The pressure gradient is at an angle $\gamma/3$ with the wall and hence for thin bubbles, where γ is small, the pressure gradient normal to the wall is small so that the boundary layer equations might still give a reasonable result.
If we start from the boundary layer equations and assume small values of u and v we can also arrive at the previous results. Here it is assumed a priori that $\partial p/\partial x$ is independent of y.
Introducing ℓ and m for the non-dimensional shear stress and curvature of the velocity profile at the wall respectively, we find

$$y_3/\theta = -3\ell/m \qquad (6)$$

Relations such as (3) through (6) are also valid with a good approximation for the Stewartson solutions with reversed flow of the Falkner-Skan equation.
In what follows we will sometimes use

$$g = y_3/\theta = -3\ell/m \qquad (7)$$

as a shape factor for velocity profiles with reversed flow near the wall.

Because the velocities in the separated region remain very small it may be expected that eq. (2) remains valid within a separation bubble at appreciable distances downstream of separation. This is illustrated by Fig. 3 in which measured streamlines from a smoke picture of a separation bubble [10] are compared to results of a calculation using eq. (2). It should be noted that the streamlines can only be calculated when γ is known. In this case the value of γ was taken from the smoke picture.

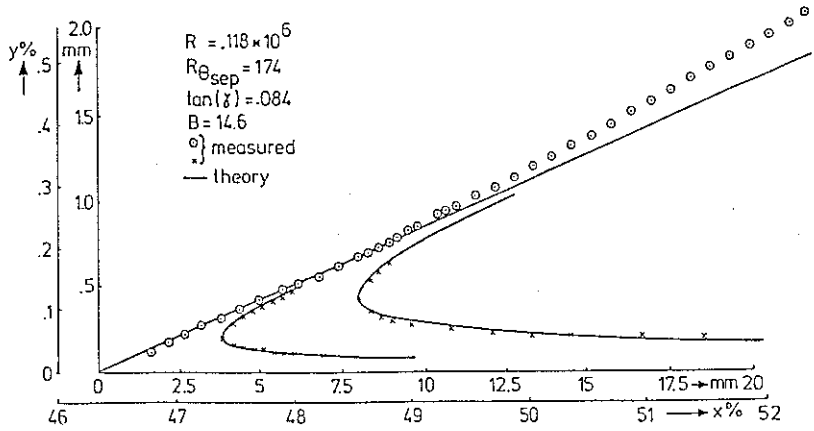

Fig. 3. Streamlines inside the laminar part of the separation bubble obtained from a smoke picture. Comparison with equation (2). Same airfoil as in Fig. 1.

3. Results of flow visualisation studies of laminar separation bubbles

When a boundary layer calculation is performed for a prescribed pressure distribution, generally the so-called Goldstein singularity will occur at separation for which the wall shear stress τ_o tends to zero like the square root of the distance to separation. In this case eq. (1) would predict a separation angle γ of 90 degrees, which is obviously in contradiction with experimental evidence. Usual ways to proceed with the calculation through the separation point, are to use the Navier-Stokes equations or at least a strong interaction model using the boundary layer equations.

An alternative way was followed at LSL, in order to develop an engineering method for the calculation of separation bubbles. An extensive series of flow visualisation studies was made in the hope that a sufficiently general empirical relation might be found from which the separation angle γ can be

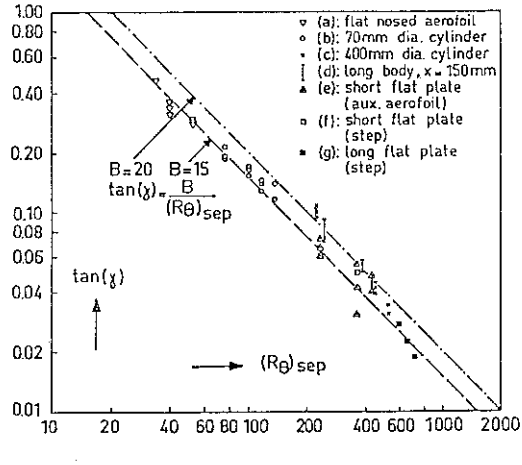

Fig. 4. Separation angle γ for various flows, [9].

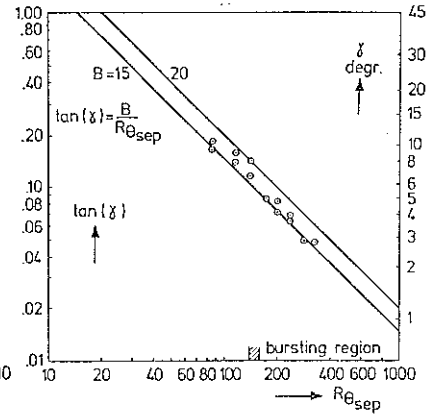

Fig. 5. Separation angle γ for the airfoil of Fig. 1 [10].

determined as a function of the boundary layer characteristics upstream of separation. Once γ is known the separated flow might be calculated using simple methods.

A first series of results has been reported in [9]. Measurements were performed on seven different model configurations in three different low speed windtunnels. The flow was made visible by means of smoke introduced into the separation bubble. The shape of the front part of the bubble was determined photographically, from which the separation angle γ could be measured.

The results are shown in Fig. 4, where measured values of $\tan(\gamma)$ are plotted vs. the corresponding value of R_θ at separation. It follows that a reasonably unique relation exists between γ and $(R_\theta)_{sep}$ which can be approximated by

$$\tan(\gamma) = B/(R_\theta)_{sep} \qquad (8)$$

with a value for the 'constant' B of about 15 to 20.

Later [10], similar experiments have been performed on a Wortmann FX 66-S-196VI airfoil; results are given in Fig. 5. For these experiments the chord Reynolds number was reduced to such low values that bursting of the bubble occurred. It follows from Fig. 5 that even after bursting relation (8) remains valid. In the LSL airfoil computer program for airfoil analysis and design eq. (8) is used with a constant mean value for B equal to 17.5.

4. Computational methods for the laminar part of the bubble

When the separation streamline for a curved wall is plotted in boundary layer coordinates, where distances are measured along and normal to the wall, respectively, the first part of the dividing streamline in the laminar part of the bubble is reasonably straight or slightly curved upwards (Fig. 3). This finding has been used [9, 10, 11] to develop a simple calculation procedure for the separated laminar flow. This method employs the Von Karman momentum integral relation and the first 'compatibility condition' of the boundary layer equations. This condition relates the curvature of the velocity profile at the wall to the streamwise pressure gradient. The following additional assumptions are made.

1. The angle γ can be determined from $(R_\theta)_{sep}$ by an empirical relation such as (8) with B = 17.5.
2. The separation streamline has a prescribed shape in the laminar part of the bubble.
3. The reversed flow velocity profiles can be represented by the Stewartson second branch solutions of the Falkner-Skan equation.

It should be observed that the pressure distribution in the separated region is not given a priori but it follows from the calculations. In other words: the pressure distribution is determined such that the assumed shape of the separation streamline is compatible with the other assumptions and with the equations used. Initial conditions which are required to start the calculation at the separation point are θ and U. These conditions follow from the boundary layer calculation upstream of the separation point.

The above mentioned method has been used for some time in the LSL airfoil computer program. The resulting pressure distributions were always found to be very similar, showing the characteristic flattening in the laminar part of the bubble (Figs 1 and 2). At a later stage, the pressure distributions have been directly derived from a universal relation which is based on a combination of experimental evidence and calculations (see chapter 5 and [4]).

Work is in progress at LSL to replace this simple engineering method with a more advanced "strong interaction" procedure as introduced by Veldman [12, 13]. In order to make the new method fast enough for design studies, where many boundary layer computations have to be made to optimise the design, use will be made of an integral method. The present rapid engineering method may be used as a first iteration to speed up convergence.

A well-known testcase for these laminar strong interaction calculations is the indented flat plate ("Carter and Wornum trough", Fig. 6). Veldman and Henkes [17] used it to show that Veldman's simultaneous calculation method

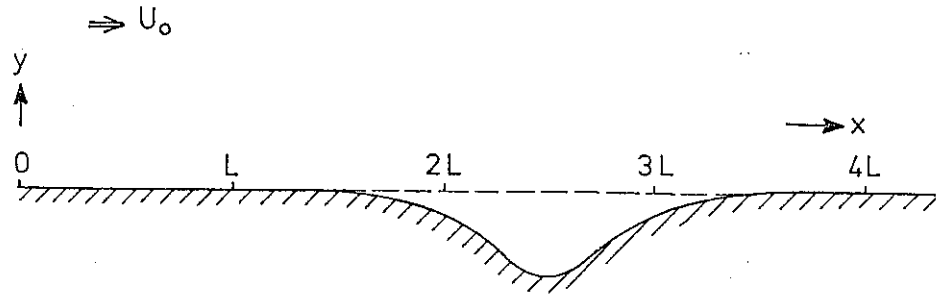

Fig. 6. Indented flat plate (Carter and Wornom) trough)
$y_{wall}/L = 2\alpha/[e^{4(\bar{x}-2.5)} + e^{-4(\bar{x}-2.5)}]$.

for the pressure distribution and the viscous flow produced good results using a finite difference method to solve the boundary layer equations. Heidsieck [14] showed that the boundary layer equations, used in Veldman's interaction scheme, give results which are in good correspondence with results of the Navier-Stokes equations. Heidsieck and Oskam [15] showed that also a treatment of strong interaction using a two-parameter integral method produced good results.
Some results due to Henkes [16] are shown in Figs. 7 and 8.
It turns out that at low Reynolds numbers the adverse pressure gradient over the trough is so much relieved by the displacement effect that the bubble disappears. It follows from Fig. 7 that the theoretical results are in a certain Reynolds number range very similar to the experimental correlations as shown in Figs. 4 and 5; only when the Reynolds number of the computations is reduced below a certain value (which depends on the depth parameter α of the trough), the bubble suddenly disappears. It is understandable that the disappearance of bubbles did not show up in the early experimental research at LSL. Observations were always restricted to flows which were forced to separate. An experimental investigation of the Carter and Wornom trough with $\alpha = -0.03$ was attempted at LSL [18]. Here the disappearance of the bubble with decreasing Reynolds number was clearly noticed. Some results of the experiments are compared to the numerical results in Fig. 8. Differences between the two sets of results may be partly due to the fact that in the experiment the pressure gradient outside the trough region was not exactly zero and even slightly favourable ($\frac{dc_p}{d\bar{x}} = -.01$ for $\bar{x} < 1$). Imposing this outside pressure gradient on the calculation leads to a shortening of the bubble with an amount $\Delta x/L = .04$.

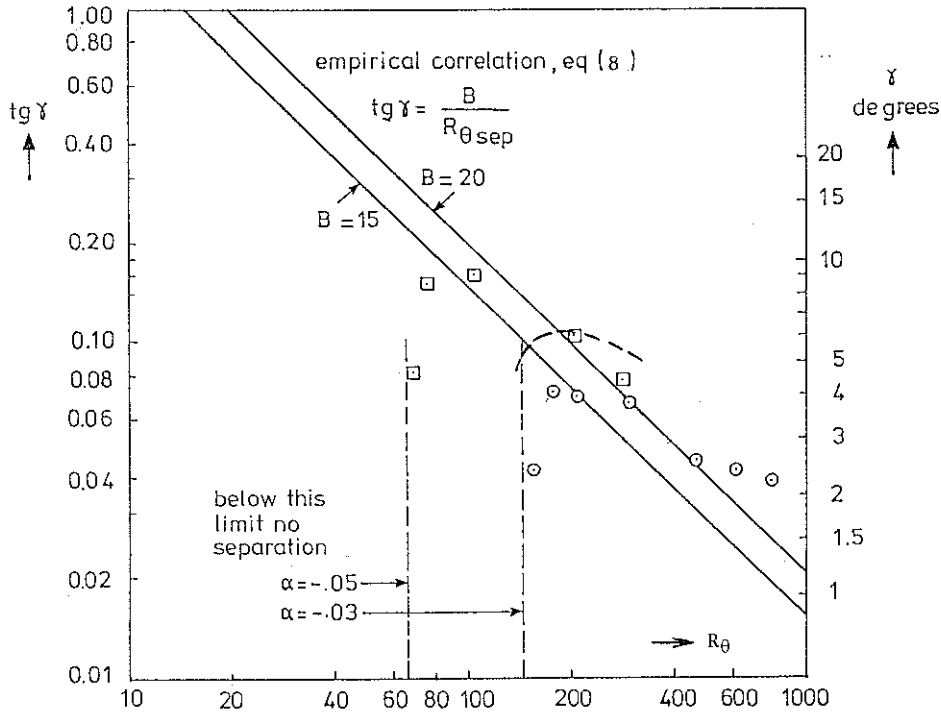

Fig. 7. Numerical results for indented plate.
⊙ $\alpha = -.03$; ⊡ $\alpha = -.05$ [16,17]; – – – $\alpha = -.03$, present one parameter method.

In future the pressure gradient will be better controlled in the experiment and taken into account in the calculations. It should be observed that it is very difficult to measure the pressure distribution accurately. To keep the flow laminar until after reattachment and to obtain a measurable separation angle the wind tunnel speed has to be kept low. In the experiment the bubble disappeared below about 3 m/s.

In order to see to what extent a simple one-parameter integral method, using Veldman's strong interaction scheme, could be used as a fast design method, the simple calculation procedure, referred to above, was modified by replacing the empirical input (assumptions 1 and 2) by Veldman's inter-

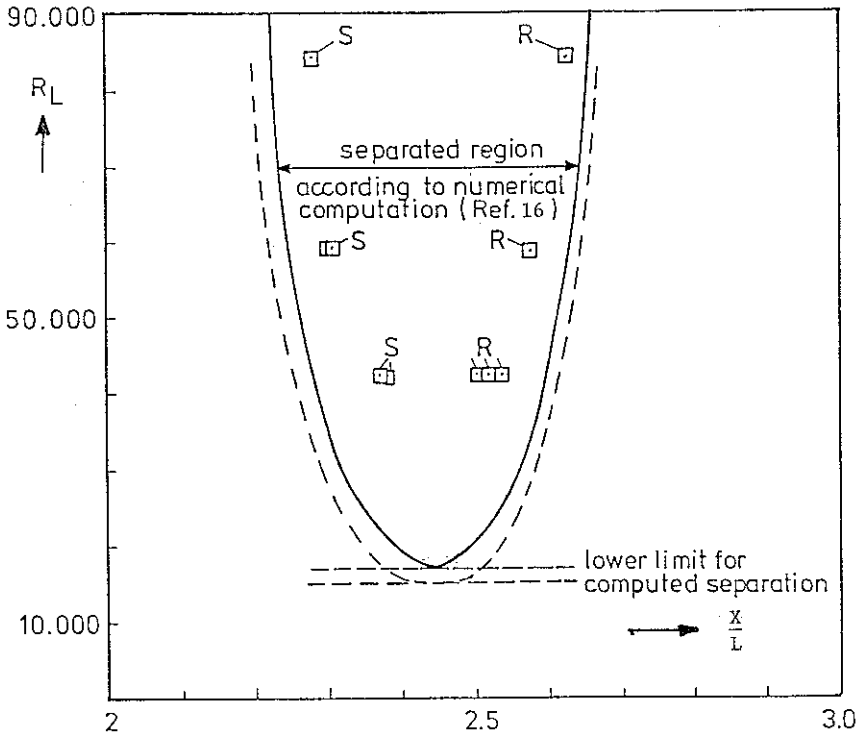

Fig. 8. Comparison between computed and experimental results for the indented flat plate. S = separation, R = reattachment, ⊡ experiment, ———[16], - - - - present one parameter method.

action scheme. Figs. 7 and 8 contain some results of this method as compared to Henkes' calculations. It follows that the present method is able to give a reasonable approximation at a much reduced computer time. It is intended at LSL to replace the present engineering method used in airfoil design by a two-parameter integral method. The present transition prediction method (section 6) will also be replaced by a two-parameter version.

5. A postulated universal description of the laminar part of the bubble

In order to arrive at a universal model of the laminar part of the bubble we start from the boundary layer equation:

$$u \frac{\partial u}{\partial x} + v \frac{\partial u}{\partial y} = - \frac{1}{\rho} \frac{dp}{dx} + \nu \frac{\partial^2 u}{\partial y^2} \qquad (9)$$

and the continuity equation:

$$\frac{\partial u}{\partial x} + \frac{\partial v}{\partial y} = 0 \tag{10}$$

It seems reasonable to assume the validity of (9) even within the separated region if only we refrain from prescribing the pressure distribution. The pressure gradient term in (9) can be related to the velocity U at the edge of the boundary layer using the Bernoulli equation.
We now make (9) and (10) non-dimensional by using θ_{sep} as a characteristic length and U_{sep} as a characteristic velocity. Taking again x as the distance downstream of separation we now define:

$$(R_\theta)_{sep} = (U_{sep}\,\theta_{sep}/\nu) \qquad \bar{y} = y/\theta_{sep} \qquad \bar{u} = u/U_{sep} \qquad \bar{U} = U/U_{sep}$$

$$\xi = x/(\theta_{sep}\,R_{\theta_{sep}}) \qquad \bar{v} = (v\,R_{\theta_{sep}})/U_{sep} \tag{11}$$

Note that in non-dimensionalizing x and v a factor $(R_\theta)_{sep}$ has been used. This is to obtain values of ξ and $\bar{v}$ with a reasonable order of magnitude and moreover to arrive at the following equations which do not contain the Reynolds number explicity:

$$\bar{u}\,\frac{\partial \bar{u}}{\partial \xi} + \bar{v}\,\frac{\partial \bar{u}}{\partial \bar{y}} = \bar{U}\,\frac{d\bar{U}}{d\xi} + \frac{\partial^2 \bar{u}}{\partial \bar{y}^2} \tag{12}$$

$$\frac{\partial \bar{u}}{\partial \xi} + \frac{\partial \bar{v}}{\partial \bar{y}} = 0 \tag{13}$$

If now we make the following assumptions:

a. U/U_{sep} is a universal function of ξ downstream of separation.
b. All velocity profiles at separation are the same when plotted as u/U_{sep} vs y/θ_{sep}.

then equations (12) and (13) and the corresponding boundary conditions are always the same, leading to a universal solution. From this it would follow that

$$\bar{U} = U/U_{sep},\ \bar{\theta} = \theta/\theta_{sep},\ y_3/\theta_{sep} \text{ and } g = y_3/\theta$$

are universal functions of ξ.
If $g = y_3/\theta$ is a universal function of ξ, then we find (note that $g = 0$ at separation):

$$\tan\gamma = \left(\frac{dy_3}{dx}\right)_{x=0} = \left(\frac{dy_3}{d\xi}\frac{d\xi}{dx}\right)_{x=0} = \frac{\left(\frac{dg}{d\xi}\right)_{\xi=0}}{(R_\theta)_{sep}} \qquad (14)$$

With $\left(\frac{dg}{d\xi}\right)_{\xi=0}$ equal to a universal constant, say B, we retrieve our experimental relation (8).

It should be stressed that the available experimental evidence to support assumption (a) is scarce and scattered. Moreover the assumption (b) is a very rough first approximation only because various separation profiles certainly show a variation of the shape factor H. Nevertheless we will proceed on this line because it will lead us to a useful frame of reference to present experimental results.

6. The e^n method for transition prediction

The e^n method for transition prediction for attached flows was developed in 1956 independently by Smith and Gamberoni [19] and Van Ingen [20]. The method was extended by Van Ingen to the case of suction [21] and separated flows [10,11].

The method employs linear stability theory to calculate the amplification factor σ for unstable disturbances in the laminar boundary layer (σ is defined as the natural logarithm of the ratio between the amplitude of a disturbance at a given position to the amplitude at neutral stability). It is found that at the experimentally determined transition position the calculated amplification factor for the critical disturbances attains nearly the same value (about 9) in many different cases for flows with low free stream turbulence levels. To include the effects of higher free stream turbulence levels, the critical amplification factor was made dependent on the turbulence level.

To obtain the critical disturbance, calculations are made for many different disturbance frequencies; the envelope σ_a of the σ-x curves for these different frequencies is used as the critical amplification factor controlling transition. Denoting the value of σ_a at transition by n, it follows that the calculated ratio of the amplitude a of the unstable disturbances to the neutral amplitude a_o is given by:

$$a/a_o = e^n \qquad (15)$$

This of course explains the name of this semi-empirical method. It is customary at LSL to use σ_a instead of n.

In linear stability theory a given two-dimensional laminar main flow is subjected to sinusoidal disturbances with a disturbance stream function:

$$\psi = \varphi(y)\, e^{i(\alpha x - \omega t)} \qquad (16)$$

For the spatial mode ω is real and α is complex $\alpha = \alpha_r + i\,\alpha_i$. This leads to a factor $\exp(-\alpha_i x)$ in the disturbance amplitude and σ follows from:

$$\sigma = \int_{x_o}^{x} -\alpha_i \, dx \qquad (17)$$

where x_o is the streamwise position where the disturbance with frequency ω is neutrally stable.

Various stability data obtained from litterature and some additional inviscid stability calculations at LSL have been reduced to a table containing about 300 numbers [10].

Using this table, the amplification rate $-\alpha_i$ can easily be obtained for any velocity profile, as soon as the critical Reynolds number is known. At LSL a boundary layer calculation method is used [10] which, for attached flow, is similar to Thwaites' method. It contains an extra parameter however, which makes the prediction of the separation position as accurate as for Stratford's two-layer method. In separated flows an integral method is used in which the shape of the separation streamline is prescribed. Both for attached and separated flow the primary profile shape parameter is m/m_{sep}. The critical Reynolds number is a function of m/m_{sep}; this function is assumed to be equal to that obtained for the Falkner-Skan solutions.

It is clear that σ is a function of x and ω for a given boundary layer; σ can be calculated as soon as stability diagrams are available for the velocity profiles for successive streamwise positions x.

Since transition occurs in a region rather than in a point, Van Ingen introduced two values of σ_a namely σ_1 and σ_2 [10] corresponding to beginning and end of the transition region. The values of σ_1 and σ_2 depend on the free stream turbulence characteristics.

Although it is clear that the initial disturbances cannot be sufficiently characterised by the r.m.s. value of free stream turbulence alone, it may be attempted to find a relation between σ_1, σ_2 and the r.m.s. free stream turbulence Tu (in %).

In many different papers relations between Tu and R_θ or R_x at transition have been given for the flat plate. The measured transition positions may be converted to σ_a-values; then σ_a will decrease when Tu increases. In [11] it is shown that, based on these flat plate results, σ_1 and σ_2 can be related to an "effective" turbulence level Tu (%) by

$$\sigma_1 = 2.14 - 6.18^{10}\log Tu \tag{18}$$

and

$$\sigma_2 = 5 - 6.18^{10}\log Tu \tag{19}$$

Application of the e^n method requires the evaluation of eq. (17) for a range of reduced frequencies $\omega\nu/U^2_\infty$; this is done on a routine basis in the LSL airfoil program. For separation bubbles a short-cut method was developed [10,11] which is thought to provide a reasonably accurate first estimate of the transition position in the separated flow at rather low values of the Reynolds number, where no appreciable amplification occurs prior to separation. This short-cut method will be described in the remainder of the present chapter.
Starting from (17) and using the non-dimensional coordinate ξ we can write (the integration starts where the specific disturbance first becomes unstable):

$$\sigma = \int -\alpha_i \, dx = (R_\theta)_{sep} \int \frac{-\alpha_i \theta}{\theta/\theta_{sep}} \, d\xi \tag{20}$$

The non-dimensional frequency $\omega\theta/U$ may be written as:

$$\omega\theta/U = (\omega \, \theta_{sep}/U_{sep})(\theta/\theta_{sep})(U/U_{sep})^{-1} \tag{21}$$

Then, using the results of chapter 5 that U/U_{sep}, θ/θ_{sep} and the shape factor may be taken as universal functions of ξ, it follows that for each frequency the integral in (20) is a function of ξ and $(R_\theta)_{sep}$. Now we make the further assumption that the Reynolds number, although low in absolute sense, is relatively high w.r.t. the critical Reynolds number so that the stability characteristics are given with sufficient accuracy by the limiting values determined from the inviscid stability equation. Then $-\alpha_i\theta$ only depends on the value of $\omega\theta/U$ and the profile parameter g but not on R_θ. Hence the integrals for the different frequencies and also the envelope are universal functions of ξ. Therefore we can write:

$$\sigma_a = (R_\theta)_{sep} \, F(\xi) \tag{22}$$

where $F(\xi)$ is a universal function of ξ which may be determined from the known relations between ξ, g and the various stability data.
A further simplification can be made when it is assumed that in first

approximation in the laminar part of the bubble θ, U and R_θ are constant and equal to their values at separation. Then constant values of $\omega\nu/U^2_\infty$ also mean constant values of $\omega\theta/U$. In the present short cut method we assume that downstream of separation g is proportional to ξ according to

$$g = B\,\xi \tag{23}$$

Hence (20) can be replaced by an integration w.r.t. g.
Similarly we can, over a short interval upstream of separation, assuming ℓ to be proportional to $x_{sep}-x$, perform the integration w.r.t. ℓ instead of x.
Hence the integration in eq.(20) can be performed once for all independently of $(R_\theta)_{sep}$ or the pressure distribution for different values of $\omega\theta/U$. From the effective turbulence level Tu the critical amplification factor follows using (18) and (19). The position of transition behind the separation point then follows from the definition of ξ and the known function $F(\xi)$.
At LSL we use this short-cut method to obtain a first estimate of the transition position only. Subsequently we always perform the full amplification calculation where also the upstream influence is taken into account. This may lead to a shorter bubble than follows from the short-cut method.
A plot of $F(\xi)$, as derived from the stability diagrams of the Stewartson velocity profiles is shown in Fig. 9. For small values of ξ we may use as a good approximation:

$$10^4\,F(\xi) = 70 + 530\,\xi \tag{24}$$

For large values of ξ we may use:

$$10^4\,F(\xi) = 491\,\sqrt{\xi} \tag{25}$$

The linear approximation (24) will be used below as a frame of reference for some further experimental results.
The square root approximation may be brought in a familiar form, which has been used by previous writers to present their experimental results. It should be noted that (25) completely neglects the amplification upstream of separation but is rather accurate for large values of ξ.
Using eq.(25) it may be shown that the position of transition x_{tr} follows from (take $x_{sep} = 0$):

$$\frac{x_{tr}}{\theta_{sep}} = \frac{237\,\sigma_a{}^2\,B\,m_{sep}}{(R_\theta)_{sep}} \tag{26}$$

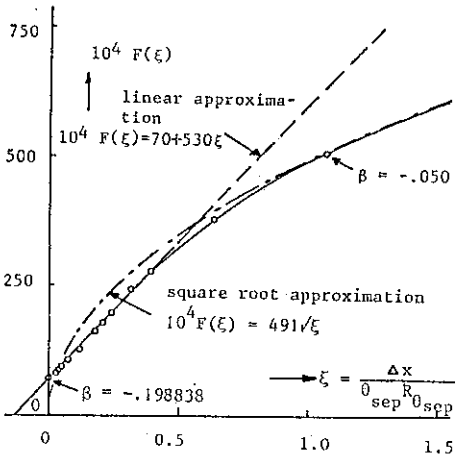

Fig. 9. The function F(ξ) and approximations (24) and (25).

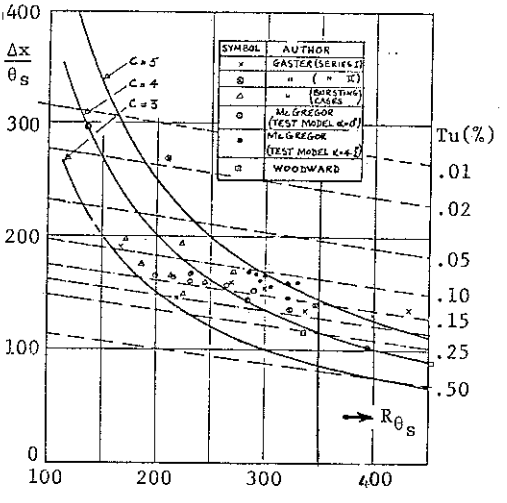

Fig. 10. The two methods of correlating experimental results for the data collected by Horton [22] ——eq.(28), - - - - eq.(30).

Using as mean values B = 17.5 and m_{sep} = 0.10 we find:

$$\frac{x_{tr}}{\theta_{sep}} = \frac{415\ \sigma_a^2}{R_{\theta_{sep}}} = .0415\ \sigma_a^2\ \frac{10^4}{R_{\theta_{sep}}} \qquad (27)$$

which is similar to a relation given by Horton [22]:

$$\frac{x_{tr}}{\theta_{sep}} = C\ \frac{10^4}{(R_\theta)_{sep}} \qquad (28)$$

with values of C ranging from 3 to 5. This range of C values corresponds to σ_a values between 8.5 and 11. It should be noted that (25) and hence (28) can only be used when transition occurs rather far downstream in the bubble; that means it is a very low Reynolds number approximation. It would lead to the unrealistic result that, with increasing Reynolds number the bubble would only disappear at infinite Reynolds numbers. At the higher Reynolds numbers it should be expected that (24) is a better approximation.

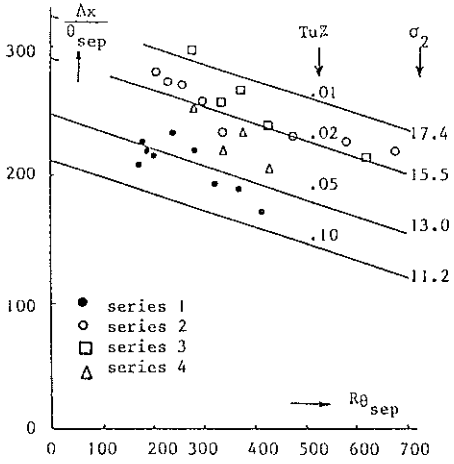

Fig. 11.

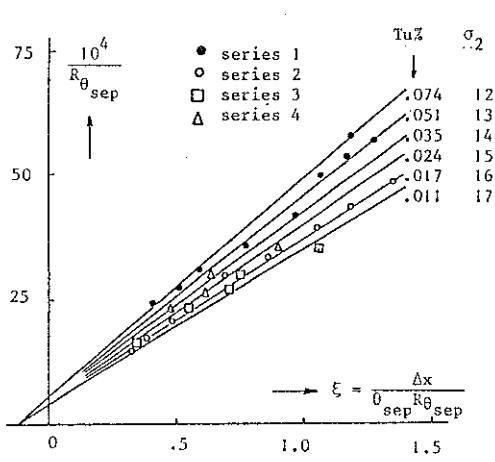

Fig. 12.

The two methods of correlating experimental results for data collected at LSL.
Series 1: Wortmann airfoil FX66-S-196 VI, α = 1 degr. in a small noisy tunnel.
Series 2: The same Wortmann airfoil but now in the large low turbulence tunnel at LSL.
Series 3: A circular cylinder with a wedge-shaped tail in the large tunnel (one of the configurations of [9].
Series 4: Same as series 3 but noise from the small tunnel recorded on tape and replayed in the test section of the large low turbulence tunnel.

The linear expression (24), together with (22) leads to

$$\frac{10^4}{(R_\theta)_{sep}} = \frac{70 + 530\xi}{\sigma_a} \tag{29}$$

Using the definition of ξ in eq. (11) this can be further reduced to

$$\frac{\Delta x}{\theta_{sep}} = \frac{10^4 \sigma_a}{530} + \frac{70}{530}(R_\theta)_{sep} \tag{30}$$

Hence, at transition, where σ_a assumes a value determined by Tu, linear relations should be observed between various characteristic parameters. Figs. 10, 11 and 12 show these relations in comparison to a number of data collected by Horton [22] and measurements at LSL [11]. In these comparisons the relation (19) between Tu and the value σ_2 for σ_a at the end of transition has been used.

It should be stressed again however that all approximations discussed in this chapter are based on the assumption that no appreciable amplification occurs upstream of separation. Only the full amplification calculation, which we use in the LSL airfoil program, will give a proper prediction of transition.

7. Concluding remarks

The present paper gives a very brief review of some aspects of laminar separation bubble research at the Low Speed Laboratory (LSL) of the Department of Aerospace Engineering at the Delft University of Technology. Due to lack of space it was not possible to discuss the reattachment problem. Neither could attention be paid to the application of this basic research to the analysis and design of airfoils for low Reynolds number applications. References [1-5] may be consulted to get a detailed overview of the work at Delft.

8. Nomenclature

The symbols used are the conventional ones. Only a few are mentioned specifically below.

g	y_3/θ; shape parameter
ℓ	$\tau_o\theta/\mu U$)
m	$-\frac{\theta^2}{\nu}\frac{dU}{dx}$
R_c	$U_\infty c/\nu$
R_θ	$U\theta/\nu$
s	distance along wall
Tu	turbulence level; %
U	edge velocity
U_∞	free stream speed
$\bar{U}$	U/U_∞ or U/U_{sep}
x, Δx	distance along wall, in general measured from separation point
y	distance from wall
y_3	y for separation streamline
γ	separation angle (Fig. 2)
θ	momentum loss thickness
$\bar{\theta}$	θ/θ_{sep}
σ	amplification factor
σ_a	envelope of σ-x
σ_1	σ_a at beginning of transition

σ_2	σ_a at end of transition
τ_o	wall shear stress

Subscripts:

S, s, sep	separation
T, tr	transition
R, r	reattachment

9. References

1. Ingen, J.L. van, Boermans, L.M.M. and Blom, J.J.H., 'Low speed airfoil section research at Delft University of Technology. ICAS-80-10.1, Munich, 1980.

2. 'Proceedings of the conference on low Reynolds number airfoil aerodynamics'. Ed. by Th.J. Mueller, University of Notre Dame, UNDAS-CP-77B123, June 1985.

3. Ingen, J.L. van and Boermans, L.M.M., 'Research on laminar separation bubbles at Delft University of Technology in relation to low Reynolds number airfoil aerodynamics', pp 89-124 in [2].

4. Ingen, J.L. van, Boermans, L.M.M.: 'Aerodynamics at low Reynolds numbers: A review of theoretical and experimental research at Delft University of Technology'. Paper nr. 1 in Proceedings of the Int. Conf. on Aerodynamics at low Reynolds numbers, October 1986, R.Ae.Soc., London.

5. Boermans, L.M.M., Donker Duyvis, F.J., Ingen, J.L. van, Timmer, W.A.: 'Experimental aerodynamic characteristics of the airfoils LA 5055 and DU 86-084/18 at low Reynolds numbers'. p 115-130 in "Low Reynolds Number Aerodynamics. Proc.Conf. Notre Dame, 1989. Springer Lecture Notes in Engineering, nr. 54, 1989.

6. Legendre, R., 'Decollement laminaire regulier;. Comptes Rendus 241, pp. 732-734, 1955.

7. Oswatitsch, K., 'Die Ablösungsbedingung von Grenzschichten'. In: Grenzschichtforschung/Boundary layer research. IUTAM Symposium, Freiburg/Br. 1957, Springer Verlag, pp. 357-367, 1958.

8. Batchelor, G.K., 'An introduction to fluid dynamics', Cambridge Univ. Press, 1970.

9. Dobbinga, E., Ingen, J.L. van, Kooi, J.W., 'Some research on two-dimensional laminar separation bubbles', AGARD CP-102, paper nr. 2, Lisbon, 1972.

10. Ingen, J.L. van, 'On the calculation of laminar separation bubbles in two-dimensional incompressible flow'. In AGARD CP-168: 'Flow Separation', Göttingen, 1975.

11. Ingen, J.L. van, 'Transition, pressure gradient, suction, separation and stability theory'. In AGARD CP-224: Laminar-Turbulent Transition, Copenhagen, 1977.

12. Veldman, A.E.P.: 'A numerical method for the calculation of laminar, incompressible boundary layers with strong viscous-inviscid interaction'. NLR-TR 79023, 1979.

13. Veldman, A.E.P.: 'New Quasi-Simultaneous Method to Calculate Interacting Boundary Layers'. AIAA Journal, 19, p 79-85, 1981.

14. Heidsieck, R.D.: 'Navier-Stokes solutions for laminar incompressible boundary layers with strong viscous-inviscid interaction'. Rept. LR-353, Delft University of Technology, Dept. Aerospace Eng., 1982.

15. Heidsieck, R.D. and Oskam, B.: 'An approximate calculation method for laminar incompressible boundary layers with strong viscous-inviscid interaction'. Unpublished work at TU Delft and NLR, 1979.

16. Henkes, R.A.W.M., 'Computation of the separation of steady and unsteady, incompressible, laminar boundary layers'. Report LR-483, Dept. of Aerospace Engineering, Delft University of Technology, 1986.

17. Henkes, R.A.W.M. and Veldman, A.E.P.: 'On the breakdown of the steady and unsteady interacting boundary-layer description'. J.F.M. 1987, vol. 179, pp. 513-529.

18. Dobbinga, E. and Ingen, J.L. van, 'Some measurements on laminar separation over an indented flat plate'. 1986 (unpublished work at LSL, Delft).

19. Smith, A.M.O., Gamberoni, N., 'Transition, pressure gradient, and stability theory', Douglas Aircraft Co., report ES 26388, 1956.

20. Ingen, J.L. van, 'A suggested semi-empirical method for the calculation of the boundary layer transition region'. Delft University of Technology, Dept. of Aerospace Engineering, report VTH-74, 1956.

21. Ingen, J.L. van, 'Theoretical and experimental investigation of incompressible laminar boundary layers with and without suction'. Report VTH-124, Delft University of Technology, Dept. of Aerospace Engineering, 1965.

22. Horton, H.P., 'A semi-empirical theory for the growth of laminar separation bubbles. A.R.C.-CP 1073, 1967.